CHAPTER 3

SOLID-STATE BATCH FOAMING PROCESS FOR MICROCELLULAR PP FOAM MANUFACTURING

3.1 Introduction

Microcellular foams are classified as a group of porous plastic materials; exhibit a very small bubble size (less than 50 μm) and with the cell density in excess of 100 million bubbles/cm^3 [45]. This interior structure of these materials influences the density reduction and the final foam properties. In addition, the use of these materials can reduce the consumption quantity of their raw material and cost-produced plastic parts without compromising mechanical properties. Due to many advantages of microcellular foams, they have been introduced in many innovative industrial applications such as lightweight and high-strength automotive parts, packaging and aerospace industries, etc [92-94]. In order to create the cellular structure in the polymeric matrix, the driving force for activation of cell nucleation sites is basically induced by the thermodynamic instability phenomena. For a batch foaming process, a solid polymer is exposed to an inert gas under high pressure [8-9, 95-99] in a pressure vessel after a sufficiently long time by mean of the polymer become supersaturated with gas. Then the polymer/gas system is removed from a pressure vessel and heated to the rubbery state [97] in order to acquire as much amorphous region as possible. In this condition, the polymer exhibits a volume expansion and a large density of nuclei [8-9, 95-99]. The earlier studies in microcellular plastics field were mainly focused on the production of amorphous

polymers such as poly(methyl methacrylate) (PMMA), polycarbonate (PC), poly(vinyl chloride) (PVC), and polystyrene (PS) [54-55, 93, 95, 97, 99]. Due to the difficulties of controlling the cell nucleation of semicrystalline polymer foams such as high density polyethylene (HDPE), polybutylene (PB), polypropylene (PP) and poly(ethylene terephthalate) (PET) [8-9, 96, 98], the study of these polymers were very challenge compared to that of amorphous polymers. The batch foaming process of semicrystalline polymers was strongly dependent on their crystal morphology and the degree of crystallinity [5, 8-9, 100-102]. Namely, the crystalline fraction of the polymer was a critical factor in the microcellular foaming process [5, 9]. Colton [103] discussed that the crystalline phase was a form of stiff region in the polymer matrix. It inhibited the gas solubility in the matrix. Therefore, in order to enhance the gas solubility in the stiff phase, the process required a high foaming temperature; closed to its melting point in order to soften the polymer and reduce the surface tension of polymer/gas system [103-104]. Moreover, the crystallinity and morphology of semicrystalline polymer can be modified by controlling the cooling rate of polymer melt [8-9, 105] and blending or contamination of another phase (impurity or additive) in the matrix [100-101, 106-108]. The cell morphology of blended foams was significantly improved compared to that of pure foams due to the presence of the dispersed phase generated the heterogeneous nucleation sites in the matrix [105]. Rachtanapun et al [100-102] supported the influence of the blending of HDPE with PP dramatically changed the crystalline morphology of polymer samples through the interfacial regions of the immiscible HDPE/PP blends which served a lower activation energy for cell nucleation. However, the cell morphology gain of the blend samples was dependent on the blend composition [100-102]. In addition, the stiffness effect of

the polymer on foaming can be suppressed by the plasticization of some additives such as gas [99] or solvent, [109] which it was found in the continuous process of foaming as the formation of polymer/gas solution [110].

Moreover, it has been found to have a research [93] that studied about the relationship between the structures and mechanical properties of microcellular foam of PVC. Tensile and impact tests were performed on the PVC foams in order to investigate the dependence of these properties on the void fraction of foamed specimens. It was found that the PVC foam with 80 % of void fraction provided the notched Izod impact strength for four times as high as that of the un-foamed PVC thereafter. Tensile strength at break deteriorated with microcellular foaming as the void fraction increased. However, the specific tensile strength was independent of the void fraction. The tensile moduli were also decreased as the void fraction increased. However, the observed tensile moduli were greater than the predicted values. Therefore, it was indicated that the relatively low density of microcellular foamed PVC can save the material and reduce the weight of the product while enhance the impact strength and reduce tensile strength and modulus to optimize a performance of the foamed materials. The study of Collias and Baird [111-112] reported that to avoid the effect of the residual gas, the property testing of the foamed samples should be conducted at least 2 weeks after the foaming.

This research was motivated to generate the microcellular structure in PP matrix through the solid-state foaming process. The home-made pressure chamber was used as the instrument for fabrication the microcellular PP foams. The conceptual design and the schematic of the process were presented in Chapter 2. The solubility parameter of chloroform is closed to that of PP [27, 32, 36]; therefore, it was selected

to use as a feasible additive to win over the effect of polymer crystallinity and also it was expected to facilitate the development of microcellular foamed structure and foaming approach. Consequently, the chloroform-plasticized procedure was introduced to the foaming method prior to the gas saturation step. The effects of chloroform and processing condition on properties of PP foams and cell morphology were investigated. The solid-state foaming process is known to have a unique advantage that it can produce very thin microcellular parts [102]. Different thicknesses (0.5 mm, 1.0 mm, and 1.5 mm) of the polymer sheet were foamed to see the effect of sample thickness on a cellular morphology. Moreover, the mechanical properties of the final PP microcellular foams such as tensile strength and impact strength were measured. However, the measurement of the notched Izod impact property was performed only at 1.5 mm of polymer thickness regarding to the requirement of the standard method (ASTM D256) of testing. The measurement of the tensile properties was done for all studied polymer thicknesses in order to see the effect of the cellular morphologies on tensile properties.

3.2 Research objectives

This experiment was proposed to produce the PP microcellular foams with different thicknesses of the polymer sheets using the solid-state batch foaming process. The advantage of the plasticization by solvent was conducted to solve the difficulty of semicrystalline PP foaming; therefore, the determination of an optimum solvent was done to select the swelling agent for using in the solvent swelling step prior to the gas saturation procedure. Then the plasticization effect of the selected solvent on the final PP microcellular foams was investigated through the crystallinity

reduction of PP sheets, cellular morphology, and the foamed properties (i.e., physical and mechanical properties).

3.3 Experimental

3.3.1 Materials

PP polymer (Moplen EP 380T SW-844), which was kindly supplied by HMC Polymers Co., Ltd., Thailand, was used to study the foaming. Its properties were listed in Table 3.1. The original melting point and crystalline fraction of the polymer pellets were measured using differential scanning calorimeter; DSC (DSC 7, Perkin-Elmer) in the range of 25-200 °C and at a heating rate of 10 °C/min to survey the processing temperature for sample preparation and foaming process. The DSC thermogram of the pellets was shown in Figure 3.1. Chloroform with 99.8 % purity was used as a solvent in the solvent swelling step. Commercial grade (99.5 % purity) of carbon dioxide was used as blowing agent in the gas saturation step.

Table 3.1 The properties of PP pellets [113].

Resin properties	EP380T SW-844
Melt flow rate (dg/min)	44
Density (g/cm^3)	0.9
Tensile strength at yield (MPa)	24
Melting temperature (°C)	169
Crystallinity (%)	36.9*

* Our experimental result

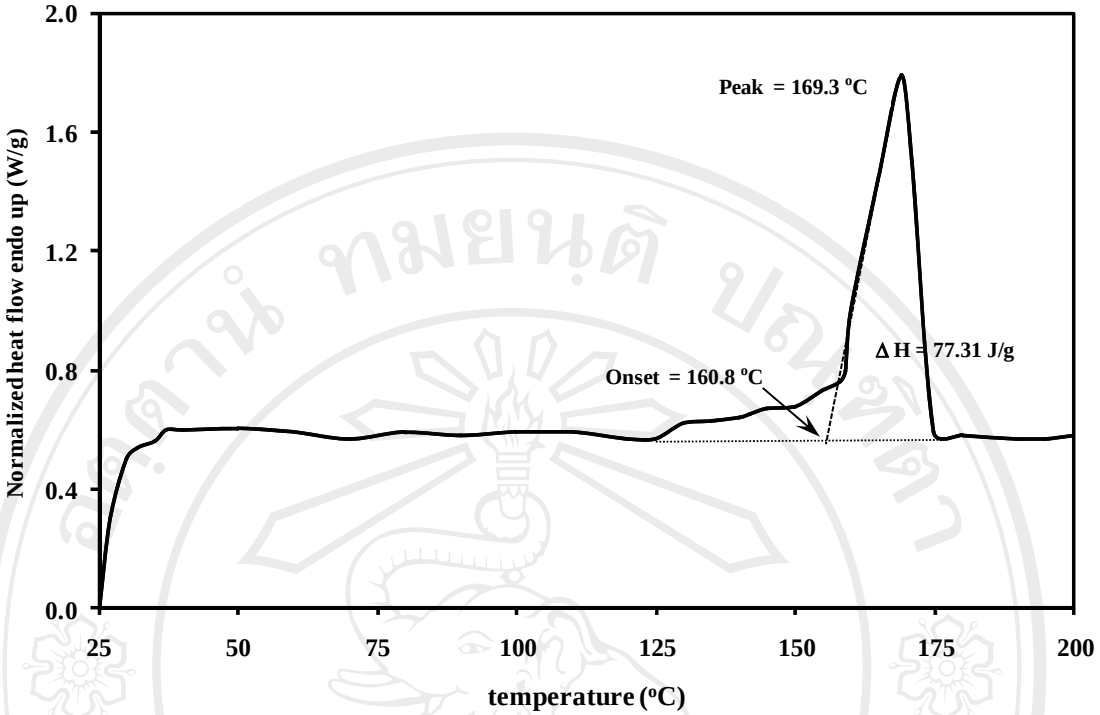

Figure 3.1 DSC thermogram of PP pellets (EP380T SW-844) in the range of 25-200 °C at heating rate of 10 °C/min analyzed by DSC7, Perkin-Elmer.

3.3.2 Sample preparation

Polymer pellets were preformed to have the different thicknesses (i.e., 0.5 mm, 1.0 mm, and 1.5 mm) by compression molding machine (Lab Tech Engineering Co., Ltd., Thailand) under a high pressure of 7.0 MPa at 185 °C for 5 minutes and the sample was cooled down at room temperature for 3 minutes. The sheet samples were cut into 2 different dimensional types (Type I: 1.25 cm × 2.54 cm and Type II: 1.25 cm × 7.00 cm). Type I samples with 0.5 mm of thickness were used to determine the absorption of solvent and the time required for the swelling step and the gas saturation step, while all thicknesses of Type II samples were used as the specimen in the foaming process. The Type I samples were subjected to easily transfer to the analytical balance, thus they were cut into the smaller size. However, in order to

investigate the impact properties of the foams the Type II samples with 1.5 mm of thickness were used as the samples in the experiment.

3.3.3 Determination of a solvent for using in the swelling step

In general, a similar or an equivalent solubility parameter of a solvent and a polymer is necessary for polymer-solvent system [27, 32, 36]. Therefore, the possible solvents with different solubility parameters such as n-hexane (14.8 $MPa^{1/2}$), tetrahydrofuran (THF; 19.4 $MPa^{1/2}$), and chloroform (18.8 $MPa^{1/2}$) [114] were selected to identify the optimum solvent that could be used in the swelling step through the determination of degree of swelling. The swelling behavior of the polymer was roughly investigated by a measurement of the mass uptake of these solvents on the polymer samples and this experiment was performed as the determination of degree of swelling [37]. Three replicates of Type I samples with 0.5 mm of thickness were immersed in chloroform at various periods of time. The mass uptakes of the samples were measured immediately at 25°C ± 2°C (lower than the boiling point of chloroform) [115] after they were taken out of the solvent bottle, and wiped out the solvent on the sample surfaces. The plot of the penetrated solvent quantities and experimental time revealed the saturated time as shown in Figure 3.2. In order to determine the saturation time for swelling the PP in chloroform, the degree of swelling of the PP at various periods of time was observed by measurement the mass uptake after immersion the polymer sheet into the solvent as described in the following section. Chloroform was found to be the best among these solvents due to it provided a higher degree of swelling than that of others; therefore, it was selected to use as a plasticized solvent for PP foaming as previously discussed.

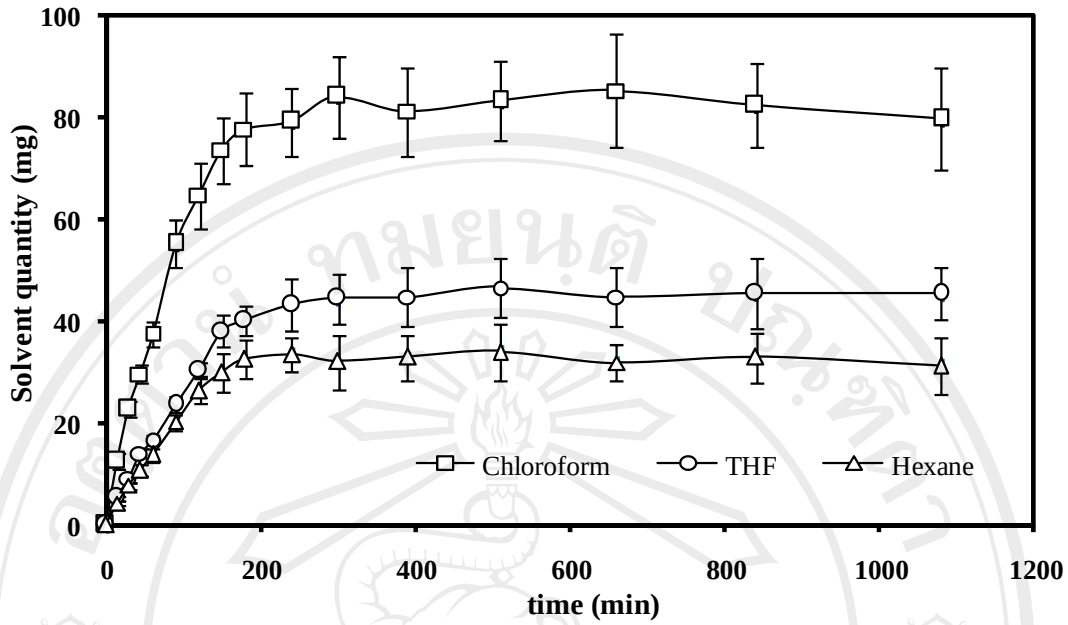

Figure 3.2 Swelling behaviors of PP sheet (0.5 mm) with various solvents at ambient condition.

3.3.4 Investigation of chloroform performance on crystallinity of PP

The effect of chloroform performance on the polymer crystallinity was investigated through the thermal analysis of PP polymer using DSC (DSC 550, Instrument Specialists Incorporated). Preformed sheet sample was denoted as “non-solvent sample” and the other was designated as “chloroform-swollen sample”. Four replicates of both samples were randomly collected by 3-5 mg. The sample was heated up from room temperature to 200 °C at 10 °C/min under N_2 atmosphere. The comparison of the DSC thermograms of both samples was elucidated as the DSC curves as shown in Figure 3.3. The crystalline fractions of both samples were calculated based on 209 J/g of heat of fusion for PP [116], and they were informed in Table 3.2.

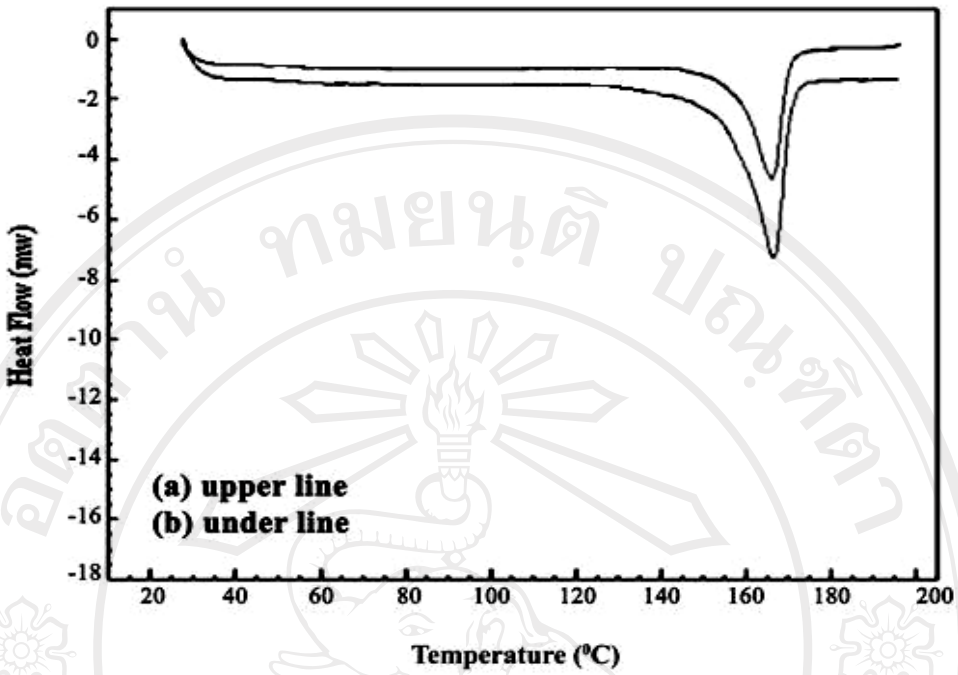

Figure 3.3 DSC thermograms of (a) Chloroform-swollen sample and (b) Non-solvent sample at 25-200 °C and the heating rate of 10 °C/min under N_2 atmosphere.

Table 3.2 Thermal properties and % crystallinity of non-solvent and chloroform-swollen samples.

Condition	Onset temperature (°C)	T_m (°C)	Heat of fusion (J/g)	Normalized ΔH (J/g)	Crystallinity (%)	Normalized Crystallinity (%)
Non-solvent samples	149	166	95.9	-	45.9	-
	151	167	92.6	-	44.3	-
	150	167	91.8	-	43.9	-
	152	166	90.2	-	43.2	-
Average	150 ± 1.3	166 ± 0.6	92.6 ± 2.4	-	44.3 ± 1.1	-
Chloroform-swollen samples	148	163	74.9	55.5	35.8	26.5
	153	165	77.9	57.7	37.2	27.6
	152	165	74.3	55.0	35.5	26.3
	154	166	76.3	56.5	36.5	27.0
Average	152 ± 2.6	165 ± 1.3	75.9 ± 1.6	56.2 ± 1.2	36.3 ± 0.8	26.8 ± 0.6

3.3.5 Saturation time of CO_2 in PP determination

The objective of this experiment was to study the absorption behavior of the blowing agent (CO_2) in the polymer matrix. In this step, three replicates of Type I samples with 0.5 mm of thickness were pressurized in a pressure vessel with 5.5 MPa of CO_2 at room temperature for various periods of time. Then samples were taken out and the weight gain of the samples was measured using the balance at 25 °C ± 2 °C and immediately recorded. The determination of gas saturation time is a widely well known method as described in many research papers [9, 76, 100, 117]. The remained amount of gas in the polymer at time (t) and the amount of gas at equilibrium state were M_t and M_∞, respectively. The diffusivity (D) for absorption was calculated using Equation 3.1 [8-9, 108].

$$\frac{M_t}{M_\infty} = 4(D/\pi)^{0.5}(t^{0.5}/l) \qquad (3.1)$$

Where, t and l were assigned as the absorption time (s) and sample thickness (cm), respectively. A plot of M_t/M_∞ as a function of $t^{0.5}/l$ yields essential a straight line (for the initial period of test) with a slope of $4(D/\pi)^{0.5}$ which is readily solved for D. In this experiment, the idea of determination of diffusivity was used to determine the saturation time of CO_2 in PP matrix. The ratios of the remained gas and polymer weight at various periods of time were plotted as shown in Figure 3.4. The plateau line and the saturation time were received from this absorption curve.

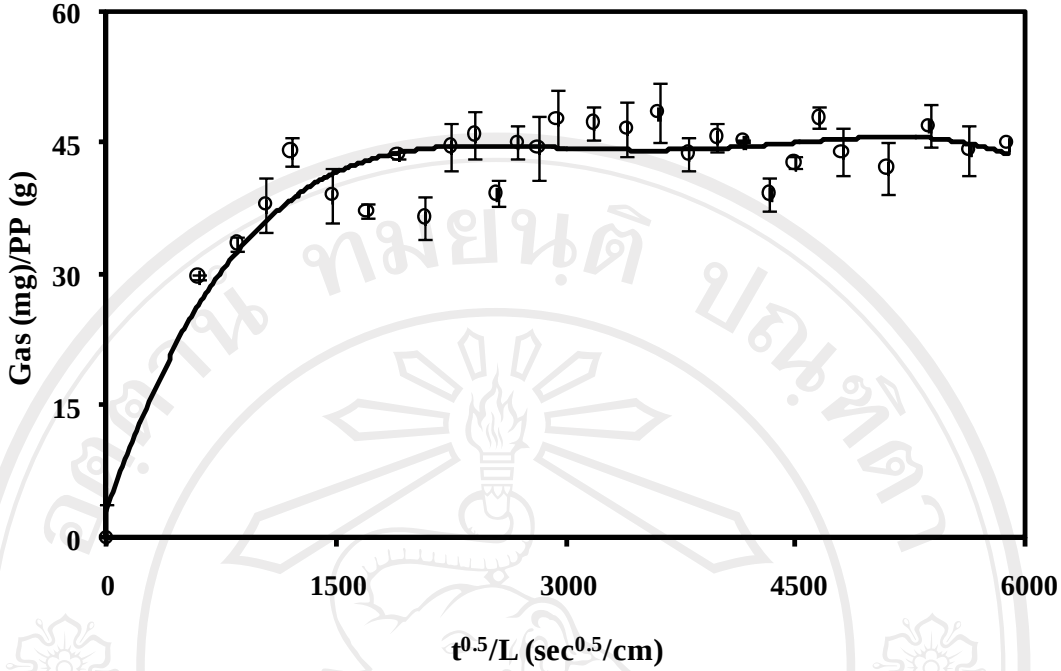

Figure 3.4 Gas absorption curve of CO_2 in PP sheet with 0.5 mm of thickness at 5.5 MPa and 25 °C ± 2 °C.

3.3.6 Foaming procedure

In this experiment, all thicknesses of Type II samples were used and they were divided into 2 sets; the first set was processed as controlled sample (non-solvent sample) and the other was immersed into chloroform for 8 hours (regarding to the solvent-saturated time in Figure 3.2) at ambient condition which was denoted as chloroform-swollen sample. After that, both samples were pressurized in a pressure vessel with CO_2 at 25 °C and 5.5 MPa for 8 hours (regarding to the gas-saturated time in Figure 3.5). The samples were removed from the pressure vessel and they were then expanded in hot glycerin oil at 4 different temperatures (50 °C, 100 °C, 155 °C, and 165 °C) for 3 seconds. In the case of foaming at room temperature (25 °C), the saturated samples were allowed to foam in the atmosphere. After the expansion,

foamed samples were suddenly quenched in a media (ethanol/distilled water = 1/1) at 23 °C to suppress the cell coalescence and wash out the residue of glycerin oil. All steps in the foaming process were set up as shown in Figure 3.5. The final foamed products of chloroform-swollen samples were studied comparatively to that of non-solvent samples in terms of the density reduction, void fraction, cell density, and average cell size correlated to the processing condition as following. Moreover, the effect of the solvent performance on microcellular foaming process and the cellular morphology of the foams with different thicknesses of PP sheets was also studied and discussed. In order to clearly see the effect of microcellular structure in the PP foams the mechanical properties such as tensile strength and impact strength were investigated and the experiment results were also discussed as the following section.

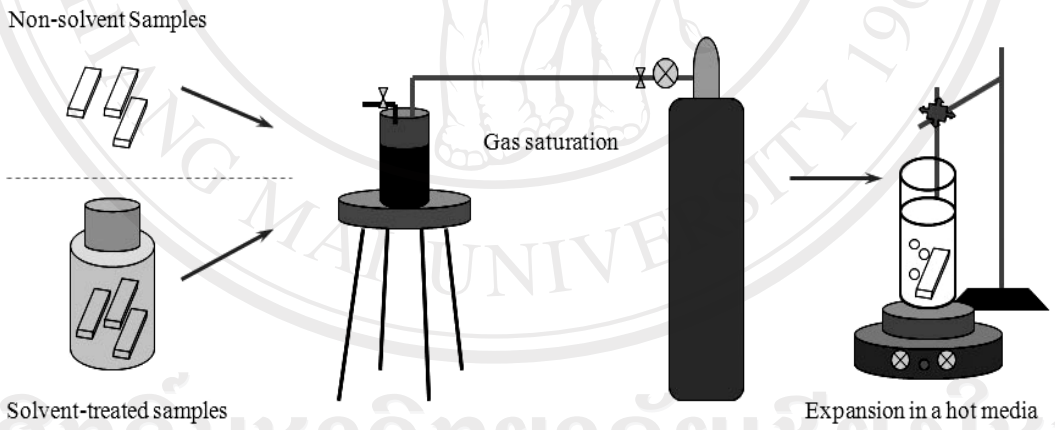

Figure 3.5 Experimental setup for solid-state batch foaming process.

3.3.7 Investigation of foam Characteristics

The effects of chloroform and processing condition on the final foam characteristics were investigated by mean of a percentage of density reduction, void fraction, cell population density, and cell size. The densities of the foams were

determined by the water displacement method as Equation 2.34 in Chapter 2, then they were calculated relatively to the initial densities of the samples in each processing conditions in order to obtain the percentage of density reduction. Consequently, the void fractions of the foams were calculated as Equation 2.35 in Chapter 2. The investigation of cellular morphologies of the foams was studied using scanning electron microscopy (SEM; JEOL JSM-5910 LV) micrographs at a magnification of 500 times. The number of cells (n) was counted in 344 cm^2 (21.3 cm $\times$ 16.1 cm) of image area. After that, the cellular morphology parameters such as cell density and average cell size were determined using Equation 2.36 and 2.39 in Chapter 2, respectively.

3.3.8 Mechanical properties testing

3.3.8.1 Tensile testing

Tensile tests were performed on a universal testing machine (LRX, Lloyd Instruments) equipped with a computer, according to the ASTM D 638 standard method. Tensile properties and data were calculated using the NEXYGEN 4.1. For each processing conditions, ten specimens (for both un-foamed and foamed samples) were tested under the strain rate of 200 $mm.min^{-1}$ by using a 2500 N capacity load cell at room temperature. However, the samples were measured under 500 N of the tensional load. The tensile properties of both samples such as tensile strength, the Young's modulus and elongation were calculated as described in Chapter 2 (Equation 2.3, 2.6, and 2.7, respectively). The elongations of the samples were calculated compared to the initial gauge length (25 mm). The Young's moduli of the samples

were measured through the ratio of stress to strain in the range of 15 % strain (below the proportional limit).

3.3.8.2 Impact testing

Naturally, PP itself has poor impact properties, especially at low temperatures. The impact properties of PP can be improved through many approaches such as an increase in toughness by the structure modification [118] and an addition of uniform small dispersed phase (< 1.0 μm) [119]. The impact properties of microcellular foams are important to their applications. In addition, the early data reported on PS foams showed several orders of magnitude improvement in the toughness of microcellular PS relative to the virgin material [120]. This could be discussed that the large numbers of small bubbles are likely to act as crack arrestors, and this will lead to an improvement in impact properties. In this experiment, the impact properties of PP foams (both chloroform-swollen and non-solvent foams) were measured compared to the un-foamed PP samples. Impact tests were performed using Impact tester TMI No. 43-1 (Testing Machine Inc., Amityville, New York) according to the ASTM D 256 Izod impact method. The impact strength of notched samples was measured through the impact energies at room temperature for fifteen specimens of each sample. In order to avoid the effect on mechanical properties of gas residues in the polymer; therefore, the property testing of the foamed samples was conducted at least 2 weeks after the foaming [111-112]. The impact strength of the samples was calculated as Equation 3.2. The specific impact strength of the sample was calculated compared to the density of the sample.

$$\text{Impact strength} = \frac{impact\ energy}{cross\ section\ area\ at\ the\ notched} \qquad (3.2)$$

3.4 Results and discussions

3.4.1 Properties of PP pellets

The crystallinity and the properties of the original PP pellets were presented in Table 3.1 [114]. After thermal analysis by DSC, the melting temperature and the crystalline fractions of PP pellets were 169 °C and 36.9 %, respectively as shown in Figure 3.1.

3.4.2 Solvent swelling behaviors of PP samples

As the results in Figure 3.2, it was found that the solubilities of all studied solvents (n-hexane, THF, and chloroform) increased as time increased but after immersion the PP sheets in the solvents more than 200 minutes the solubilities trended to level off. Among these solvents, chloroform was found to be the best in the amount of absorption; therefore, it was selected to use as a plasticized solvent for PP foaming. Moreover, the solubility curve of chloroform revealed the time required for swelling the polymer. Therefore, 8 hours of saturation time was selected to perform on the swelling step. It was found that for more than 12 hours of sample immersed in chloroform, partly dissolution of the polymer into the solvent was occurred which yield the weight reduction of the polymer.

3.4.3 Effect of chloroform on thermal property and crystallinity of PP

The foaming process of semicrystalline polymer usually requires a high temperature near its melting point [103]. Moreover, the thermal property investigation of a plastic material was necessary as a basic data for a polymer forming. Therefore, thermal properties of PP were determined by DSC in order to use these values as a basic information in the foaming process. The melting temperature (T_m) of the original polymer pellets was 167 °C with ≈ 37 % of crystalline fraction. As the results in Figure 3.3 and Table 3.2, the crystallinity of non-solvent sample was increased to ≈ 44 % due to the secondary crystallization (heat annealing) [121] in sample preparation step. After the samples were soften by chloroform the crystalline fraction was significantly reduced to ≈ 27 % as the smaller amount of heat of fusion (normalized ΔH_m) at the melting temperature of the sample (56.2 J/g of polymer) as shown in Table 3.2. This is because chloroform can act as a plasticizer and separate the chains apart, so the decreasing of the order of polymer chain fold is obtained, which is the same as it was reported for the blending effect [100-102] or the performance of fast cooling rate in quenching step [8-9]. The influence of heterogeneous sites were induced to facilitate the foaming ability of PP resin by using some additives or contamination of secondary phase as well as blending of another component into the main polymer matrix. The heterogeneity makes the matrix to be soft to contribute the increasing of gas solubility. Since the stiffness of the polymer was reduced as the interfacial regions occurred, the bubbles with microcellular characteristics could be nucleated [100-102, 105-108]. Therefore, chloroform was selected to increase the stiffness loss in PP resin and the performance of this solvent had been investigated. The crystalline fraction of chloroform-swollen samples was lower than that of non-

solvent samples about 39 %. Moreover, the melting temperature of chloroform-swollen samples was slightly lower than that of non-solvent samples. Although, the crystalline reduction of the PP matrix could be occurred by using of chloroform as the result from DSC analysis, but the influence of chloroform on the crystallinity needed to be further studied by other methods such as WAXS, etc. However, the DSC result could show the change in the polymer matrix which was swollen by chloroform compared to that of non-solvent PP sample. Namely, the order of polymer chain fold was lowered by the penetrated chloroform then the polymer matrix was soften and eased the gas absorption and foaming of PP.

3.4.4 Saturated time for CO_2 absorption in PP

According to the diffusivities of blowing agent in each polymer are not equal; therefore the gas absorption curve has been studied to determine the gas saturated time prior to the foaming process [8-9, 95-99, 100-101, 108]. After the gas solubility was eventually converged to a steady state, it was then represented the constancy of gas solubility in the polymer [8-9, 108]. As the result in Figure 3.4, the plateau revealed the gas saturation time, which was about 8 hours. Therefore, the samples were exposed to CO_2 gas for 8 hours before foaming process.

3.4.5 Effects of chloroform and processing condition on density and void fraction

After the investigation of physical properties and morphology of final foams, the samples (non-solvent and chloroform-swollen samples) possessed the different results significantly. The experimental results showed the temperature dependence of the density reduction and the void fraction. They increased when the

foaming temperature increased due to the dissolved gas can easily be diffused into the polymer matrix at the elevated temperature [90]. The research of Rachtanapun *et al*. [101-102] revealed that the cell morphology of pure PP samples was developed when the foaming temperature was increased to 175 °C. At low temperatures (i.e., 135 °C or 160 °C), the cellular structure could not located in the polymer matrix due to the temperature was lower than the melting point of PP. Despite, foaming the samples above the melting temperature potentially improved the morphology and void fraction in the matrix; however, the cellular structure was not uniform. This is because the crystallinity effect and the hindrance of polymer sheet thickness could not contribute the uniform-cell nucleation and uniform heat transfer through the sample. Therefore, a large cell size was only nucleated on the surface area of the sample, while the center of sample was not foamed. However, it was found that microcellular structure was developed in the subsurface. It was reported that an introduction of the secondary phase into PP matrix was possible to increase a crystallinity loss in the PP regions due to a low viscosity of another phase, and resulted too soft material, which was too soft to maintain the microstructure [101-102]. Our experimental results showed that the utilizing of chloroform-swelling step prior to the gas saturation procedure could facilitate the enhancement of the void fraction as Figure 3.6. Chloroform acted as a plasticizer, which located between polymer chains and made the chain far apart. Therefore, the reduction of crystallinity was observed as informed in Table 3.2. Figure 3.6 shows the tendency of void fraction which was respected to the increasing of the foaming temperature. For foaming of PP sheets with 0.5 mm and 1.0 mm of thicknesses at 25 °C and 50 °C, the void fraction of chloroform-swollen samples was 7-10 %, compared to 3-5 % when foaming the samples without chloroform at the

same thickness. But at these low temperatures, the change in void fraction of the foams was not clearly seen in the thicker sheets (1.5 mm). This might be because these temperature ranges (25 °C and 50 °C) did not provide the 1.5 mm-PP matrix to be soften enough to obtain a large number of cells and increment of void fraction as shown in Figure 3.6. Foaming at the temperatures higher than 100 °C showed the theoretical increment in the void fraction as the temperature increased and it was higher than that of foaming at low temperatures for 25 °C and 50 °C about 76-93 %. In addition, chloroform-swollen samples provided an increasing of void fraction at all foaming temperatures comparatively to that of non-solvent samples. It can be said that a high void fraction of the final foam would be achieved without the deformation of polymer and cell sacrifice (cell coalescence) at high foaming temperature when including of the solvent swelling step to the foaming procedure. It can be seen that including solvent-swelling step was superior than blending other phase into PP in term of foaming. Because the accomplishment of blending approach with the same amount of void fraction had to be processed at higher foaming temperature (i.e., 160 °C or 175 °C) for a longer period of time, while our studied method gave the same quality of foamed product at a lower foaming temperatures (25 °C or 50 °C). Moreover, the blended ratio of all components was a crucial factor to contribute the nucleation area for the uniformity of fine-celled foams.

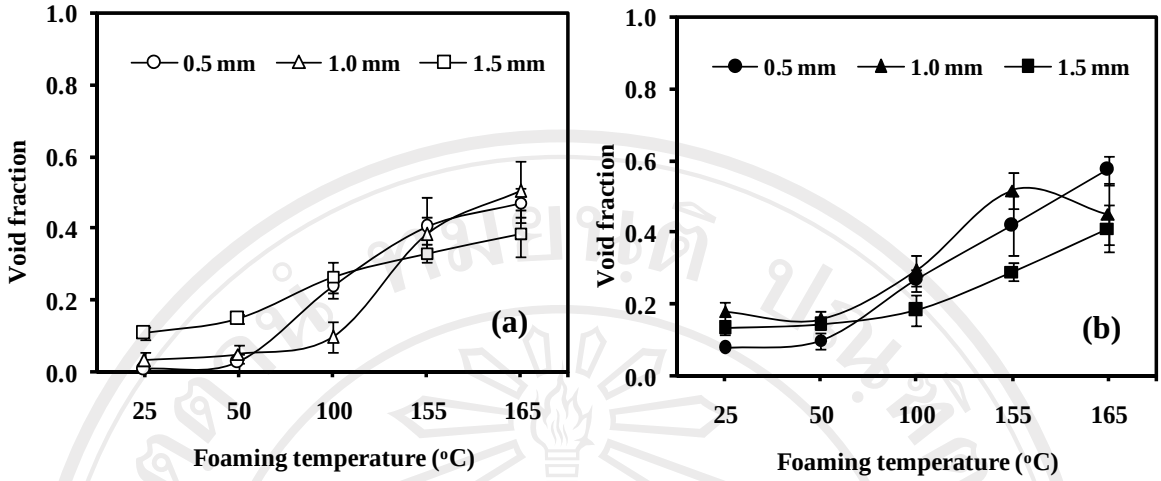

Figure 3.6 Void fraction of PP foams with various thicknesses at various processing conditions; (a) Non-solvent foams and (b) Chloroform-swollen foams.

3.4.6 Effects of chloroform and processing condition on cell morphology

It is well known that it was very difficult to receive a uniform microcellular structure in the solid-state foaming process when a polymer had a high crystalline fraction; which inhibited the gas absorption in the matrix [5, 8, 103]. However, the stiff phase of the polymer could be modified by various methods as previously mentioned [101-103]. After modification of the polymer matrix, the crystalline phase was shifted to amorphous phase resulted the reduction in crystalline fraction. A uniform cell distribution with a large number of cell nucleation was then promoted due to the ease of gas solubility in amorphous regions [5, 100-101, 106-109]. It was reported that for HDPE/PP blend, even at the foaming temperature above its melting point, the cellular structure was developed only at the sub-surface but not the center [101-102]. However, the uniform cell distribution and microcellular structure could be developed when chloroform was used to overcome the hindrance of crystallinity in PP microcellular foaming as the results of this research. In the case of

chloroform-swollen samples with 0.5 mm of thickness the uniform distribution of micro-cell number was increased regardless the elevated foaming temperature; which a high cell density ($\approx 10^{10}$ cells/cm^3) could be obtained by using the temperature only at 25 °C or 50 °C. On the other hand, to receive the same amount of cell density for the case of foaming without the solvent-swelling step the samples required a high foaming temperature (i.e., 100-165 °C) to generate a high density of nuclei. This is because the crystallinity of the polymer inhibited the gas solubility in the matrix [5, 8, 103]. Moreover, the cell-to-cell diffusion of blowing agent was accelerated easily under a high temperature. Since the blowing agent diffused through cell wall of the adjacent cells then the cells coalescence phenomena resulted in larger cells in the final foams [90] as shown in Figure 3.7 (c)-(e). Likewise allowing the samples to expose with chloroform prior to gas saturation step, fine cell size (in the range of 3-8 μm) and uniformity of isolated foams were successfully achieved for all foaming temperatures as shown in Figure 3.7 (f)-(j). Though chloroform-swollen samples seemed to exhibit some big bubbles at the temperatures in the range of 100 °C to 165 °C but the interconnected cells did not located in the polymer matrix as the case of non-solvent sample (noticeable circle areas) as shown in Figure 3.7 (c)-(e). It could be discussed that an introduction of chloroform-swelling step in the foaming procedure was very effective to create a large cell-population density and microcellular PP foams due to the effect of plasticization and the heterogeneous nucleation site generation by dissolved chloroform in the matrix. In addition, a high density of micro cells without the cell coalescence could be achieved regardless the foaming temperature for 0.5 mm-PP foams. The cell morphology of final foams was investigated using SEM micrograph, cell density and average cell size of all samples increased as the foaming

temperature increased and they exhibited the cell density in the range of 10^8-10^{10} cells/cm^3 with a small cell size of 3-8 μm as shown in Figure 3.8-3.9.

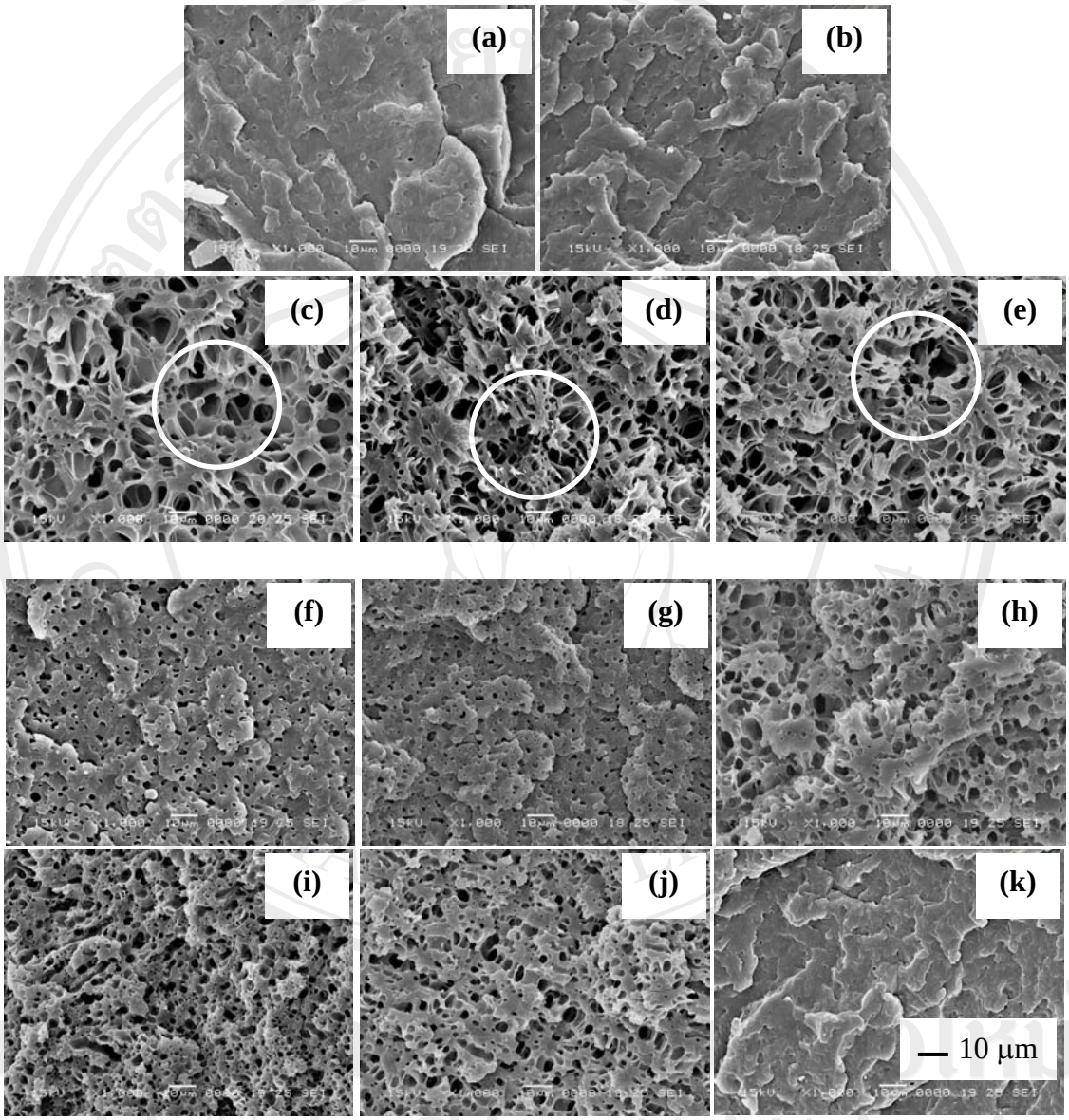

Figure 3.7 SEM images of PP foams (0.5 mm) at 1000 times of magnification;

(a)-(e) Non-solvent PP foams at 25, 50, 100, 155, and 165 °C, respectively.

(f)-(j) Chloroform-swollen PP foams at 25, 50, 100, 155, and 165 °C, respectively.

(k) Un-foamed PP sheet.

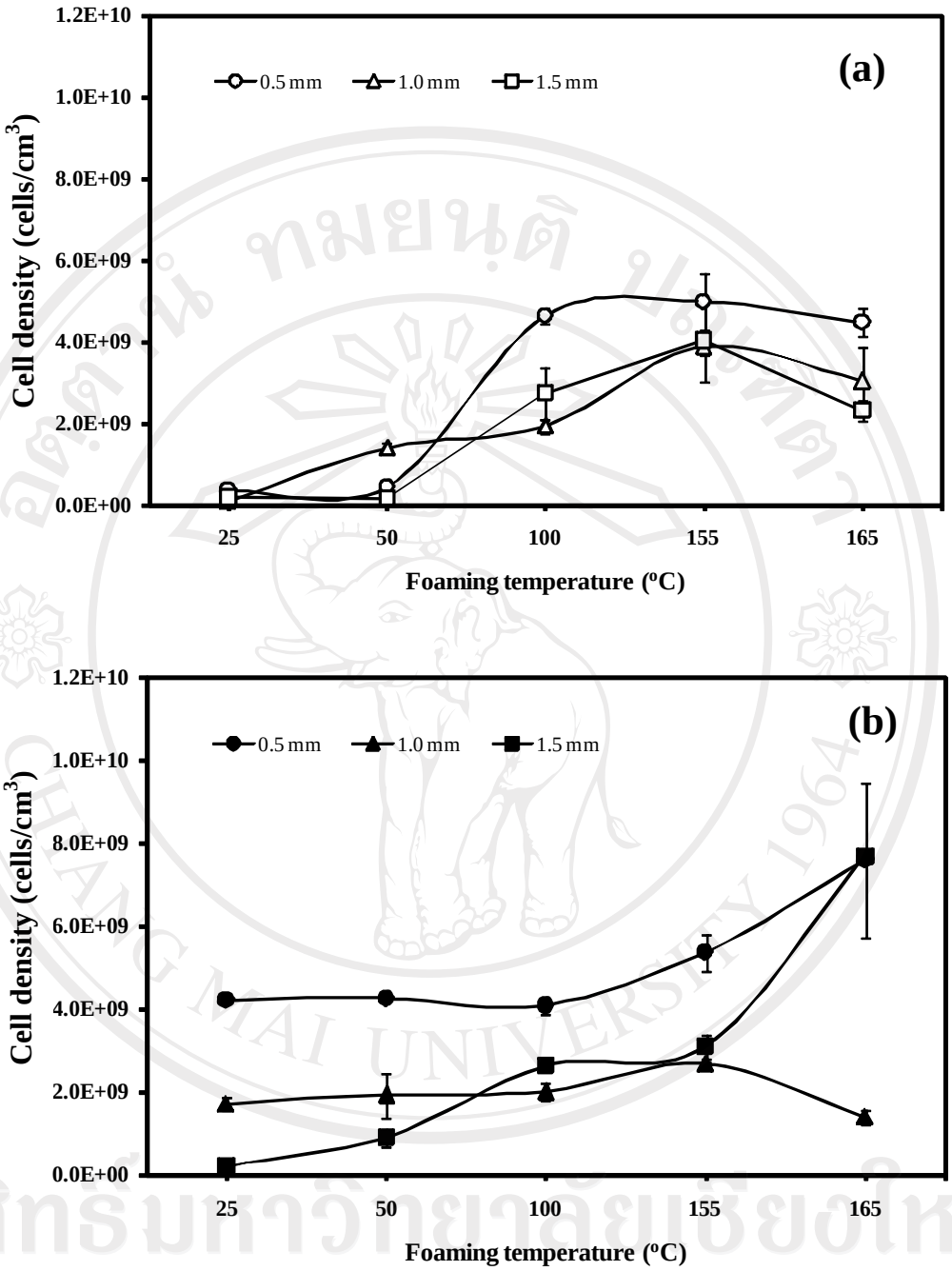

Figure 3.8 Cell densities (cells/cm^3) of PP foams with various thicknesses at various processing conditions; (a) Non-solvent foams and (b) Chloroform-swollen foams.

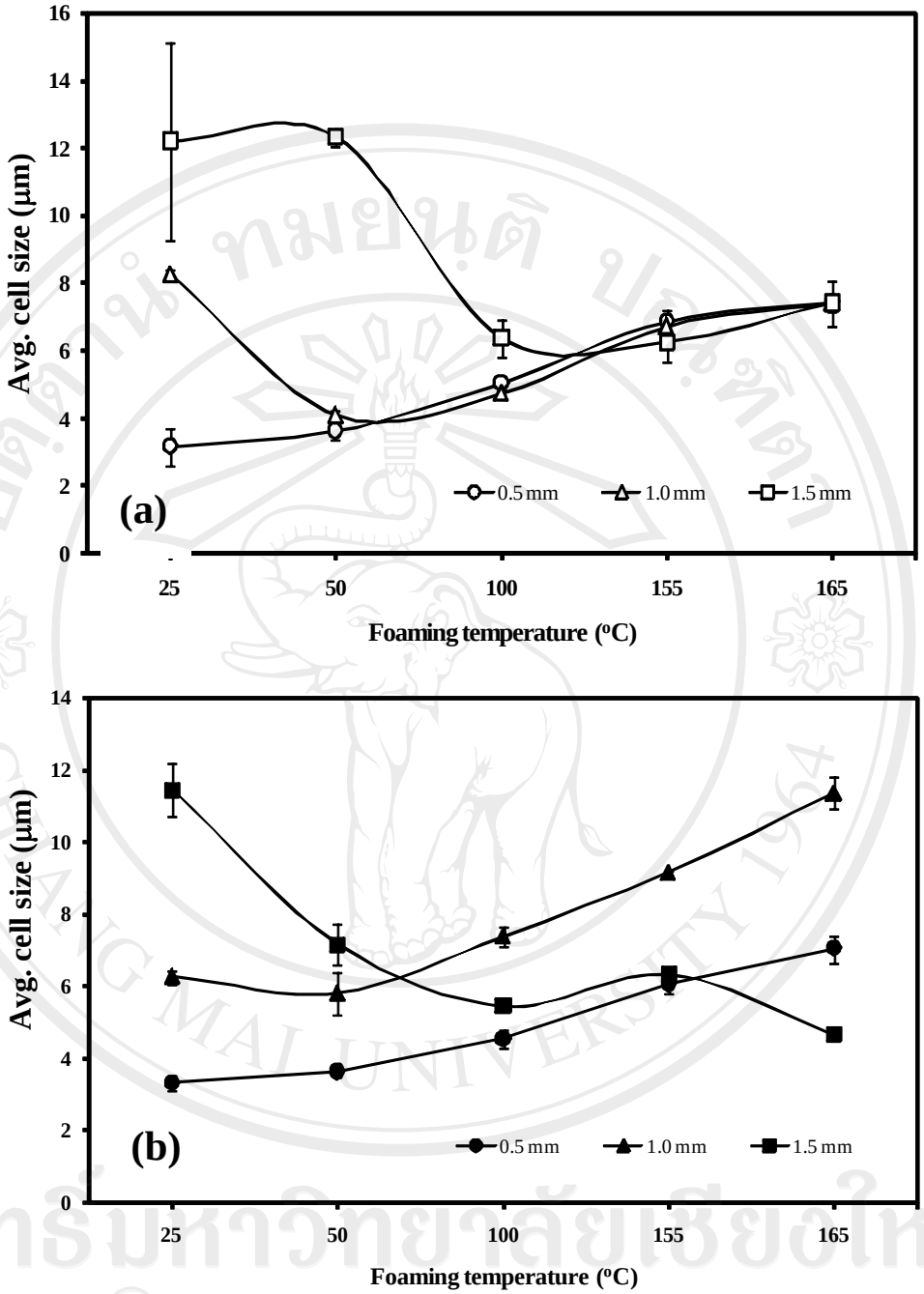

Figure 3.9 Average Cell size (μm) of PP foams with various thicknesses at various processing conditions; (a) Non-solvent foams and (b) Chloroform-swollen foams.

However, it was found that the effect of thickness seemed to slightly influence the foamability and density reduction of the foamed samples, especially when foaming the samples at low temperatures (i.e., 25 °C and 50 °C) as shown in Figure 3.10.

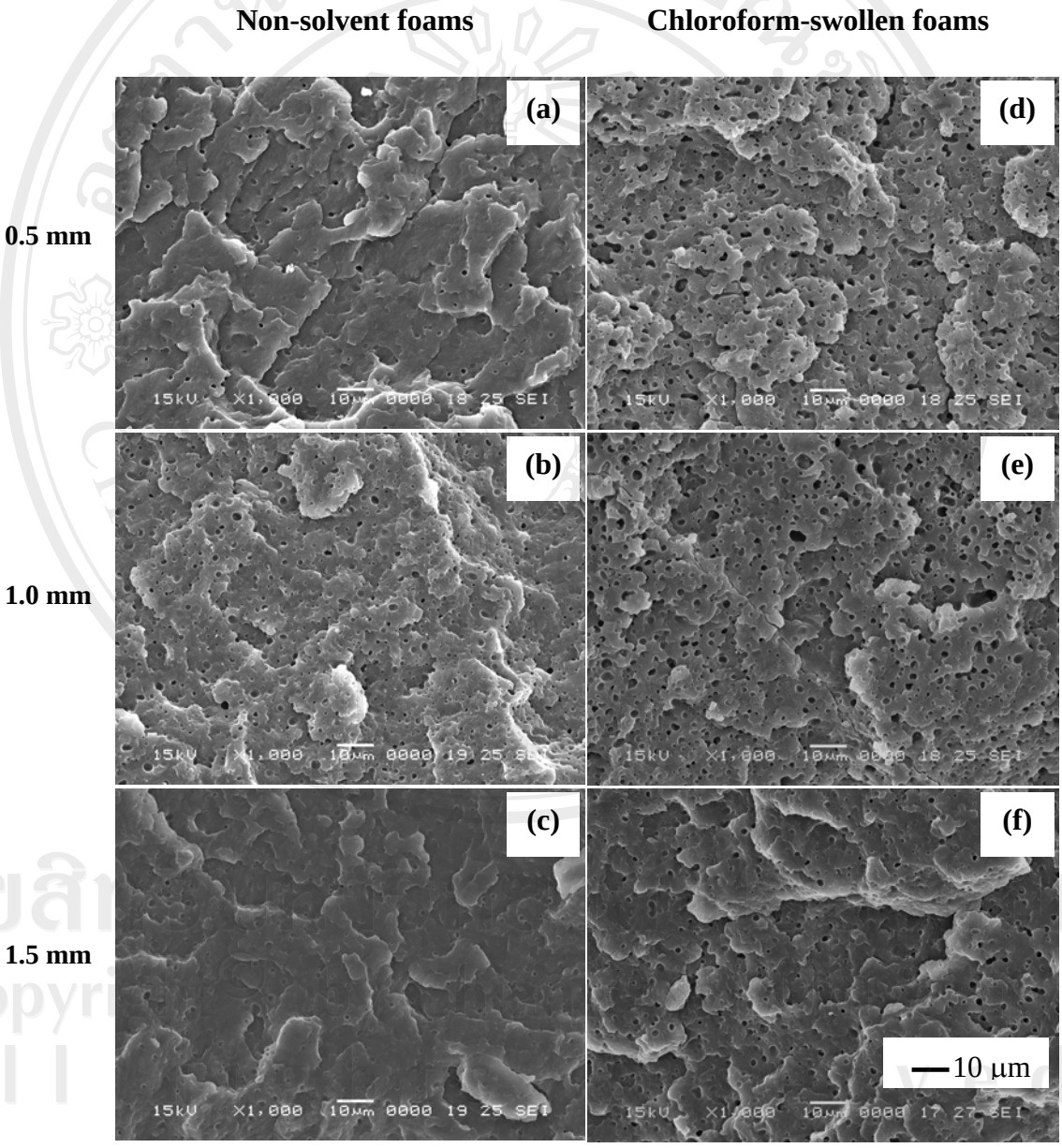

Figure 3.10 SEM images of (a)-(c) non-solvent foams and (d)-(f) chloroform-swollen foams at 50 °C, 1000 times of magnification.

In addition, the thickness effect of the foamed samples was negligible when the temperature was gradually raised. As the result in Figure 3.8 (b), the plasticization effect of chloroform can serve the foamability of the thick samples for all foaming temperatures and this effect could be clearly seen in the case of foaming with 0.5 mm-PP sheet at 25 °C and 50 °C. This was due to the plasticized solvent could enhance the soften phase of PP matrix to facilitate a very high bubble nucleation. According to the ease of gas diffusion into a thin sheet (0.5 mm), a very high amount of cell nucleation could be generated compared to that of a thicker one (1.0 mm and if it is 1.5 mm) due to the difference of the heat transfer through the polymer with different thickness. The amount of gas that can diffuse into a thicker sheet was less than that of thin sheet. However, the chloroform-swollen foams with 1.5 mm of thickness exhibited a higher amount of cell density than that of the 1.0 mm-thick foams at 155 °C and 165 °C. This might be because foaming at these temperatures, the penetrated solvent in a thicker sheet could be evaporated and act as a blowing agent to generate the bubbles in the matrix due to its low boiling point. Therefore, a high amount of cell density in a thicker sheet could be achieved. On the other hand, the evaporation of the solvent was not occurred when foaming at 25 °C and 50 °C thus the effect of the polymer thickness showed an important role on the cell nucleation behavior. Furthermore, it was found that cell densities of non-solvent foams with 1.0 mm of thickness seemed to be higher than those of chloroform-swollen foams at high temperatures but their cellular structure was non-uniform and the bubbles were only promoted at the subsurface of the foams as shown in Figure 3.11 (a). For chloroform-swollen foams, it can be seen from Figure 3.11 (b) that the uniform foam could be generated all over the specimen.

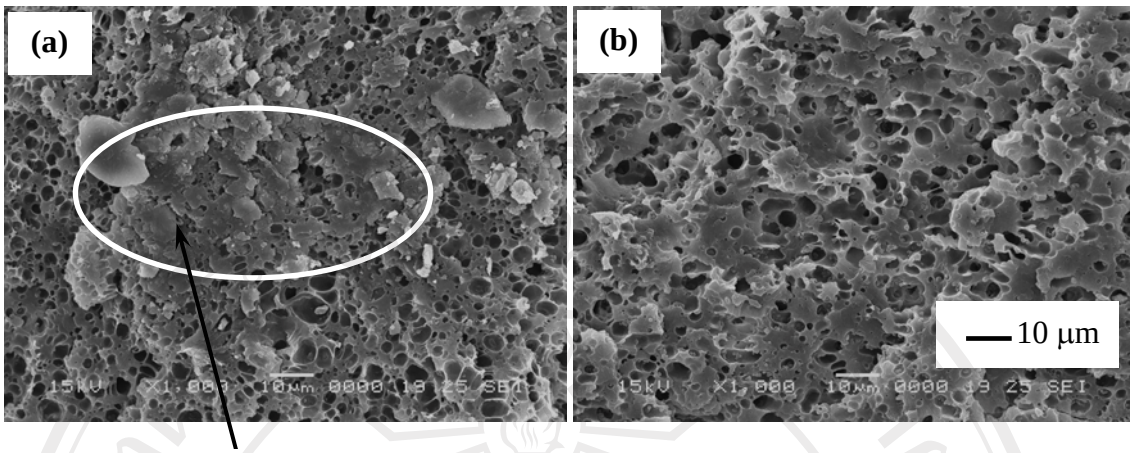

Figure 3.11 SEM images of (a) non-solvent foams and (b) chloroform-swollen foams at 155 °C (1.0 mm in thickness), 1000 times of magnification.

According to the results of cell density, the thickness of the samples seemed to be an important factor on the foamability at low temperatures. Inversely, when all samples were performed at a higher temperature a higher amount of bubbles could be generated then the effect of foaming temperature could play more dominant factor on the foamability instead of the effect of the sample thickness as shown in Figure 3.12.

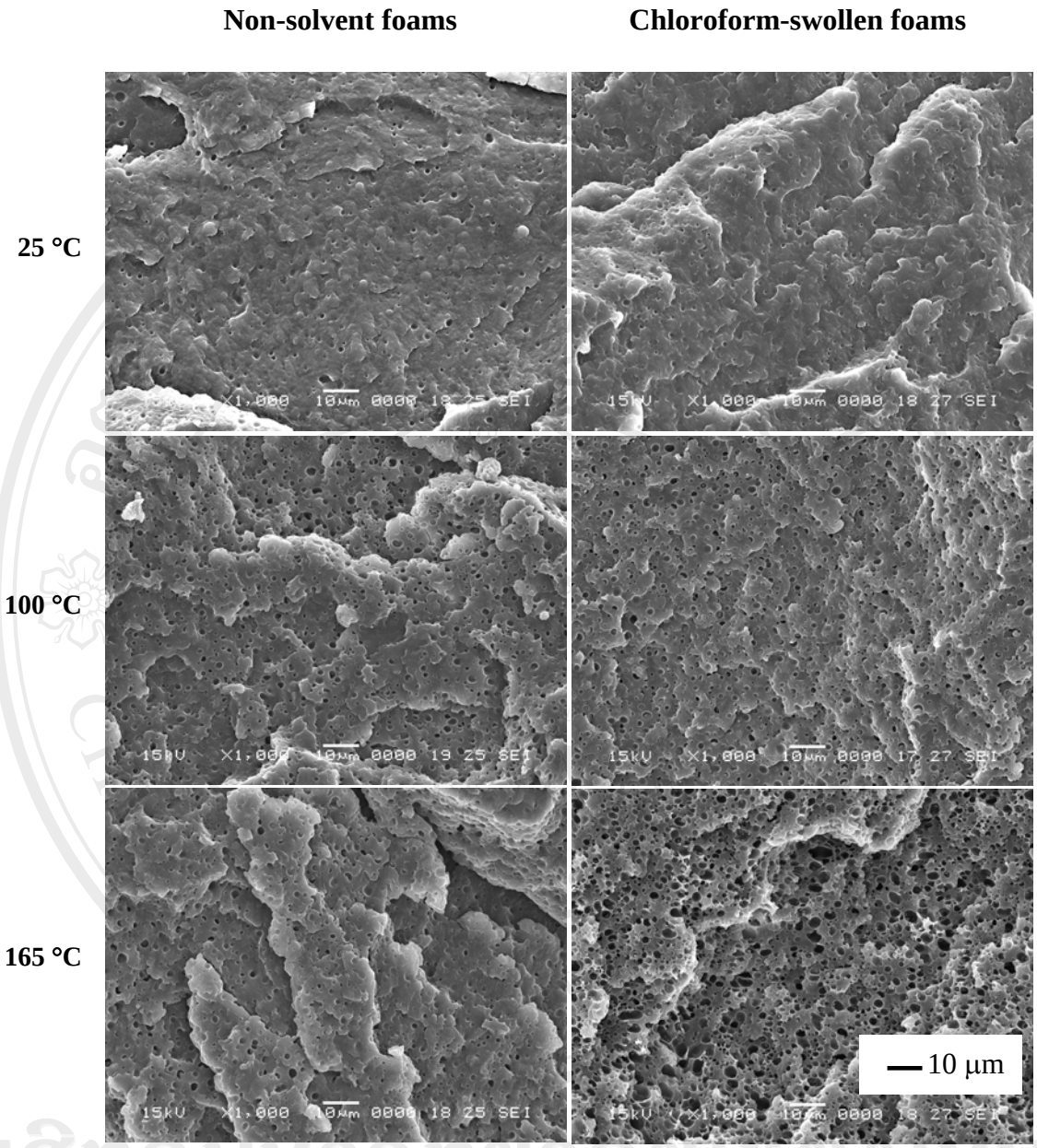

Figure 3.12 SEM images of PP foams with 1.5 mm of thickness at 1000 times of magnification.

As the previously mention, the foaming temperature played an important effect on the cell nucleation when foaming at high temperature. At this temperature, the solvent worked incorporation with the temperature and it behaved as a chemical

blowing agent during the expansion step. However, when foaming at low temperature, the polymer was not soften enough to facilitate the nucleation and the nucleation behavior of the PP matrix was strongly affected by the sample thickness. These phenomena could be observed on the cell size of the foams. As the results in Figure 3.8 and 3.9, a bigger cell size of the final foams was observed when a small amount of bubbles was nucleated on the polymer matrix as the case of foaming at low temperatures. This was clearly seen in the case of foaming without the solvent-swelling step. The reason for this was because the nucleation of the cells in the PP matrix at low foaming temperature did not facilitate the high amount of nuclei; therefore, the cells was able to be growth as much as they can in the polymer matrix without the interruption of the adjacent cells. Therefore, the foams with a small amount of nucleated bubbles would have a bigger cell size. On the other hand, when the samples were performed at a high temperature, the density of cells which nucleated in the matrix was very high due to the reduction of the stiff phase in the polymer matrix and the heterogeneous nucleation of the cells through the evaporation of the solvent. Consequently, the foams, those were allowed to expand at a high temperature (or the temperature that closed to the melting point of the polymer), provided a high cell density and smaller cell size.

3.4.7 Effects of foaming conditions on the mechanical properties

3.4.7.1 Tensile properties of PP foams

After the final foams were performed under the tensional load using the universal testing machine, the tested properties such as tensile strength at a maximum load, elongation, and Young's modulus were discussed relatively to the cellular

morphology and the physical properties of the final foams. The representative stress-strain curves for each processing condition were shown in Figure 3.13-3.15. The stress-strain curves (Figure 3.13-3.15) showed the characteristics of the samples under the tensional force versus the foaming conditions. The un-foamed samples exhibited a high tensile strength and showed the hard characteristics (high stress and medium strain) as shown by the dot-line curve. It was clearly observed in the case of samples with 1.0 mm and 1.5 mm of thicknesses. The un-foamed sample with 0.5 mm of thickness showed a less tensile strength than those of the 1.0 and 1.5 mm thick samples. This might be because during the compression molding, a higher amount of PP pellets is used to prepare the thick sheets so the internal pressure may be higher and make the polymer sheet become denser compared to the processing of thin sheet. This shape of curve was also found in the case of the PP foams at low foaming temperatures such as 25 °C and 50 °C because these foams were composed of small amount of cell density. However, most of the curves of PP foams seemed to be broader than those of un-foamed samples. This was due to the cell walls could be more elongated by the tensional force during the tensile test and they made the polymer matrix became ductile. This characteristic was clearly shown in the foamed samples which were composed of a high density of the cells. Thus, the foamed samples would present the ductility and toughness as the case of PP foams at high temperatures (100 °C-165 °C) as could be seen by the curves (purple, pink, and blue line) in Figure 3.13-3.15.

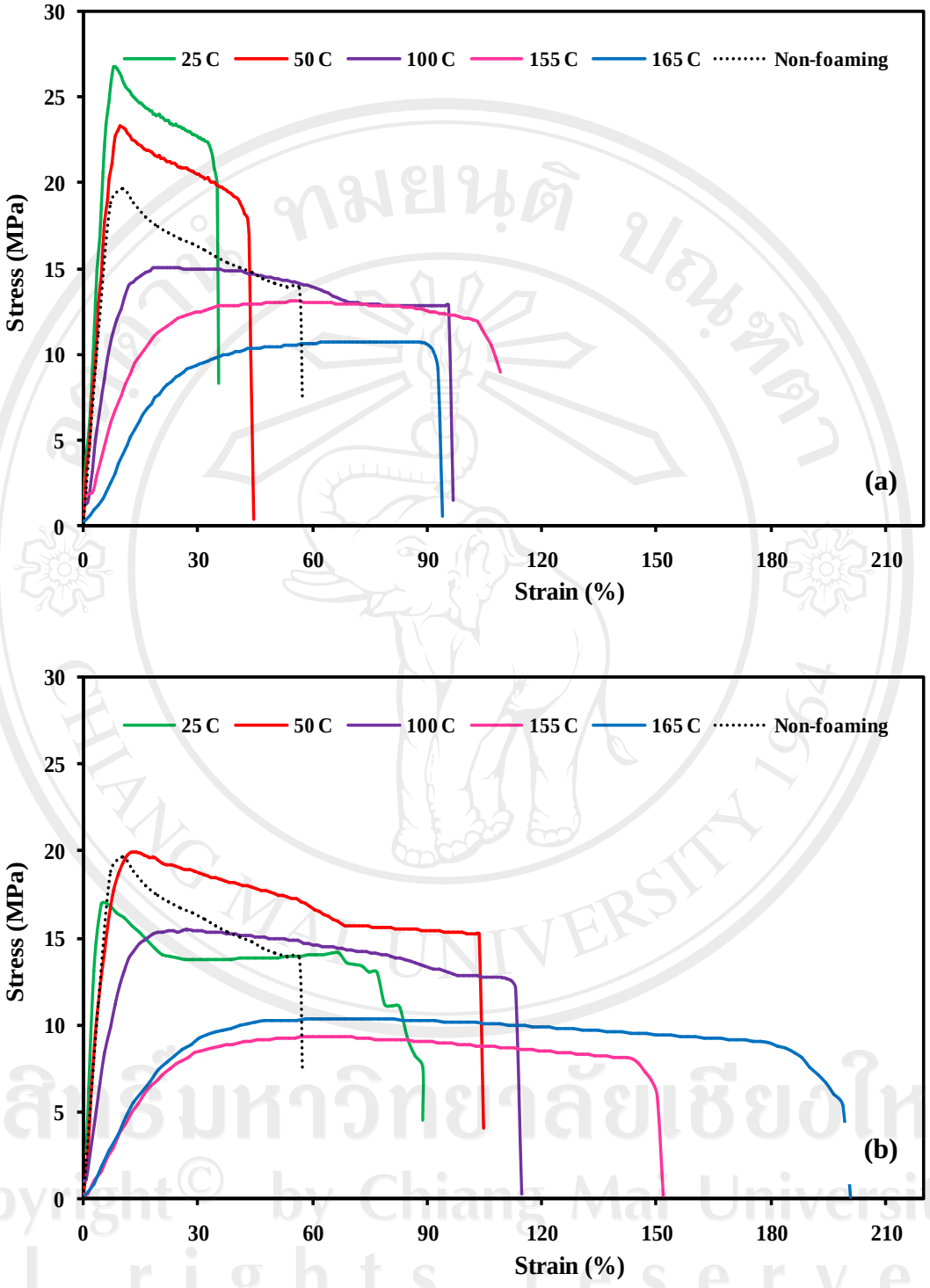

Figure 3.13 Stress-strain curves of all samples with 0.5 mm of thickness at various foaming conditions (a) non-solvent foams and (b) chloroform-swollen foams.

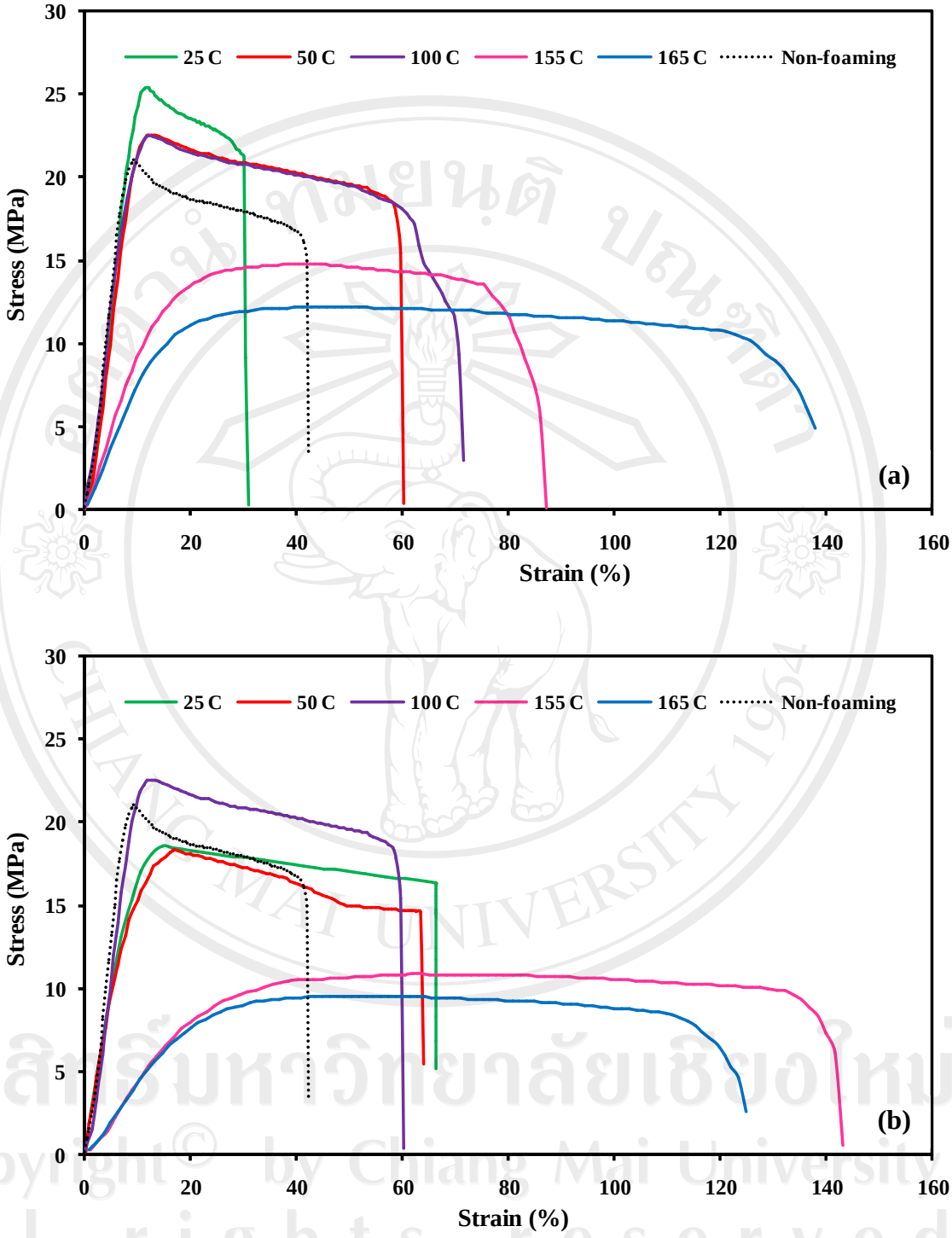

Figure 3.14 Stress-strain curves of all samples with 1.0 mm of thickness at various foaming conditions (a) non-solvent foams and (b) chloroform-swollen foams.

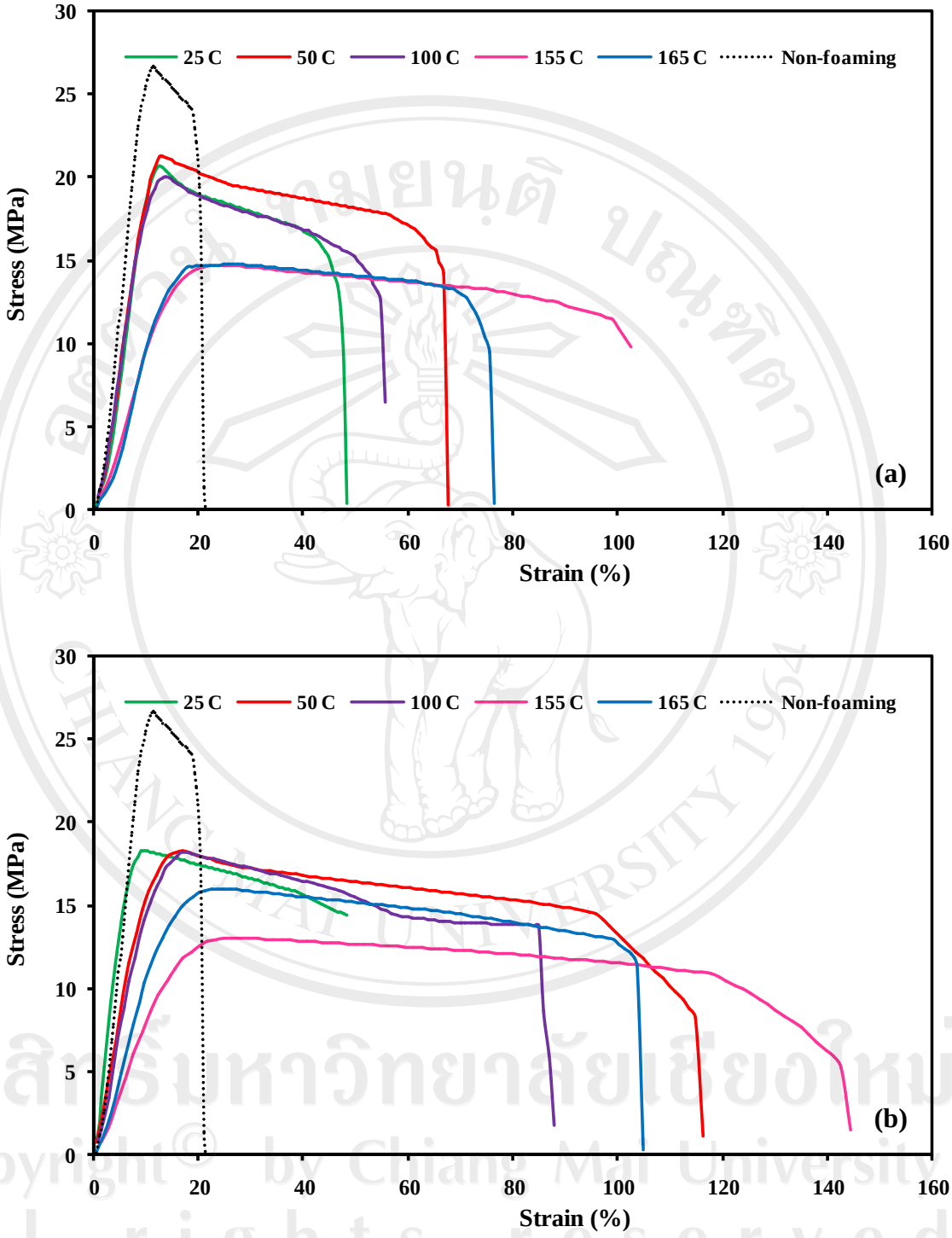

Figure 3.15 Stress-strain curves of all samples with 1.5 mm of thickness at various foaming conditions (a) non-solvent foams and (b) chloroform-swollen foams.

Consequently, the relationship between the tested properties and the processing condition of all studied samples were investigated through the results in Figure 3.16-3.18. Figure 3.16 (a) showed an increment of tensile strength of un-foamed sheets was increased as sample thickness increased and the strength values were increased from 20 MPa (for 0.5 mm of thickness) to 25 MPa (for 1.5 mm of thickness). In general, forming the polymer using the compression molding the overcharge of polymer pellets are used to ensure that the polymer melt can fully fill in the mold. At this condition, the flash can increase the pressure inside the mold and made the polymer sheets dense. Therefore, the compressed-polymer sheets which were prepared to be thicker, the amount of the polymer pellets could contribute an increased pressure inside the mold during the compression and made the polymer sheets more dense as previously discussed. The tensile strength of the foams seemed to be decreased as the void fraction increased as could be seen in Figure 3.16 (b)-(d). All foamed samples provided the tensile strength dependent on the foaming temperature. Namely, the strength of the foams was decreased as the foaming temperature increased. The strength values were significantly dropped from 20-25 MPa to 10 MPa, approximately when compared to un-foamed samples at all sample thicknesses. This was because the presence of a high void fraction in the foamed samples as could be described by Equation 2.33 in Chapter 2. This equation expresses that the void fraction is a function of the ratio of foamed density and the density of un-foamed sheet. This means that when the foamed samples have low density they will have a very high void fraction as resulted in less tensile strength. In addition, non-solvent foams provided higher tensile strength compared to that of chloroform-swollen foams due to a smaller amount of cell density. However, the tensile strength

of chloroform-swollen foams with 1.5 mm of thickness at 165 °C was not affected by the foaming temperature as resulted in the closed value of the strength of the same thickness of chloroform-swollen foams at other foaming temperatures. This was because at this processing condition provided the finer cell size with a high cell density as the results in Figure 3.8 (b) and 3.9 (b).

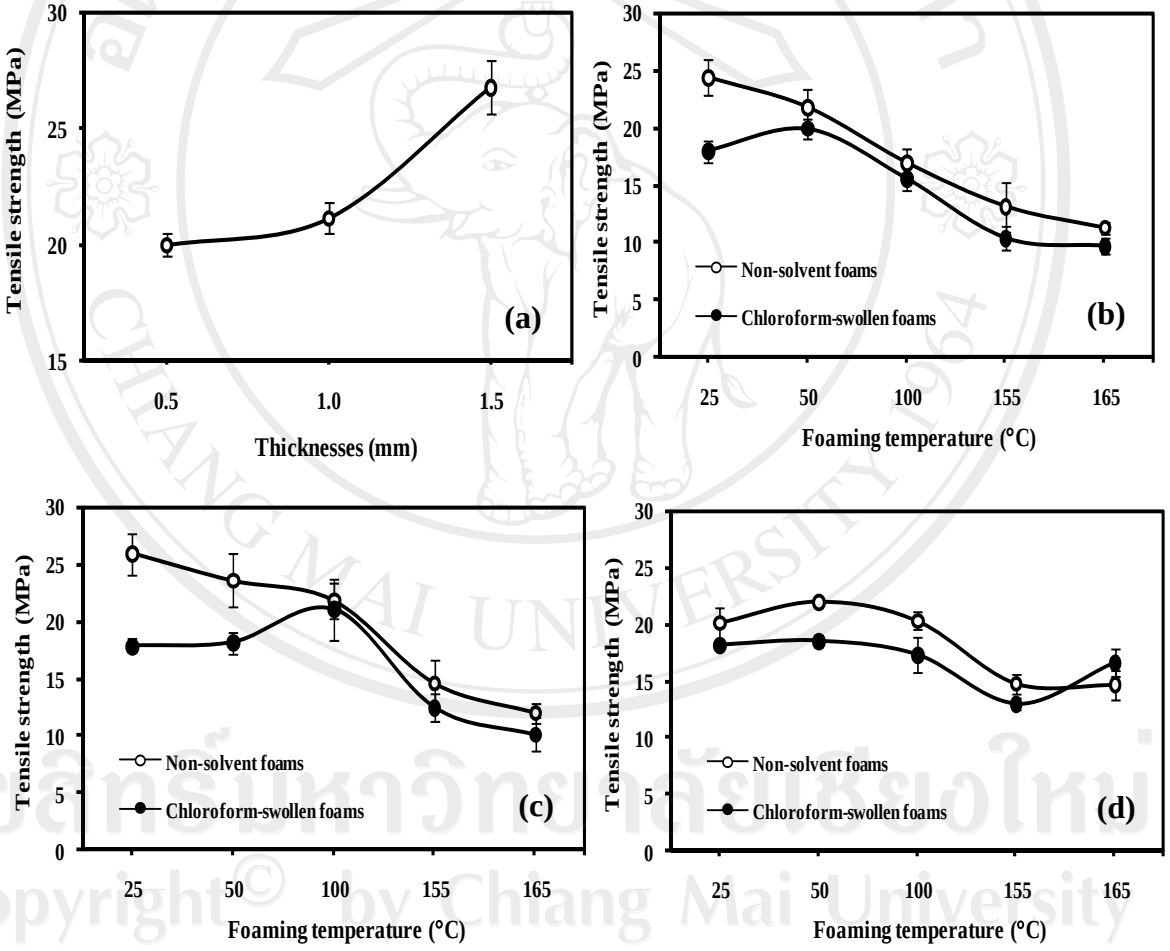

Figure 3.16 Tensile strength at maximum load of all samples at various foaming temperatures; (a) Un-foamed sheets (b) PP foams with 0.5 mm (c) PP foams with 1.0 mm, and (d) PP foams with 1.5 mm.

Although, the tensile strength of the foams was changed due to the sample thickness as previously discussed but the elongations at the maximum load were not affected by the thickness of the sample as shown in Figure 3.17 (a). However, it was found that the foams were elongate as the increasing of foaming temperature due to the increase of void fraction of the foams. It was obviously observed in the foams with the thicknesses of 0.5 mm and 1.0 mm, as shown in Figure 3.17 (b) and (c). When foaming at high temperatures (155 °C or 165 °C), the elongations were increased about 3-5 times compared to un-foamed samples and the foams which were foamed at low temperatures (25-100 °C). In addition, the elongation values of chloroform-swollen foams were slightly higher than those of non-solvent foams due to a higher amount of void fraction (or cell density) as the results show in Figure 3.7. This might be because when the voids were initiated in the polymer, the denseness of the polymer was less and promoted the flexibility of the foams. On the other hand, when foaming the 1.5 mm-PP sheets, the elongations of the foams were not dramatically changed compared to the un-foamed samples at the same thickness. However, when foaming the foams with 1.5 mm of thickness at the temperatures (155 °C or 165 °C) which closed to the melting point of the polymer, a high number of cells could be nucleated through the softening phase as resulted in the slightly increased elongation as shown in Figure 3.17 (d).

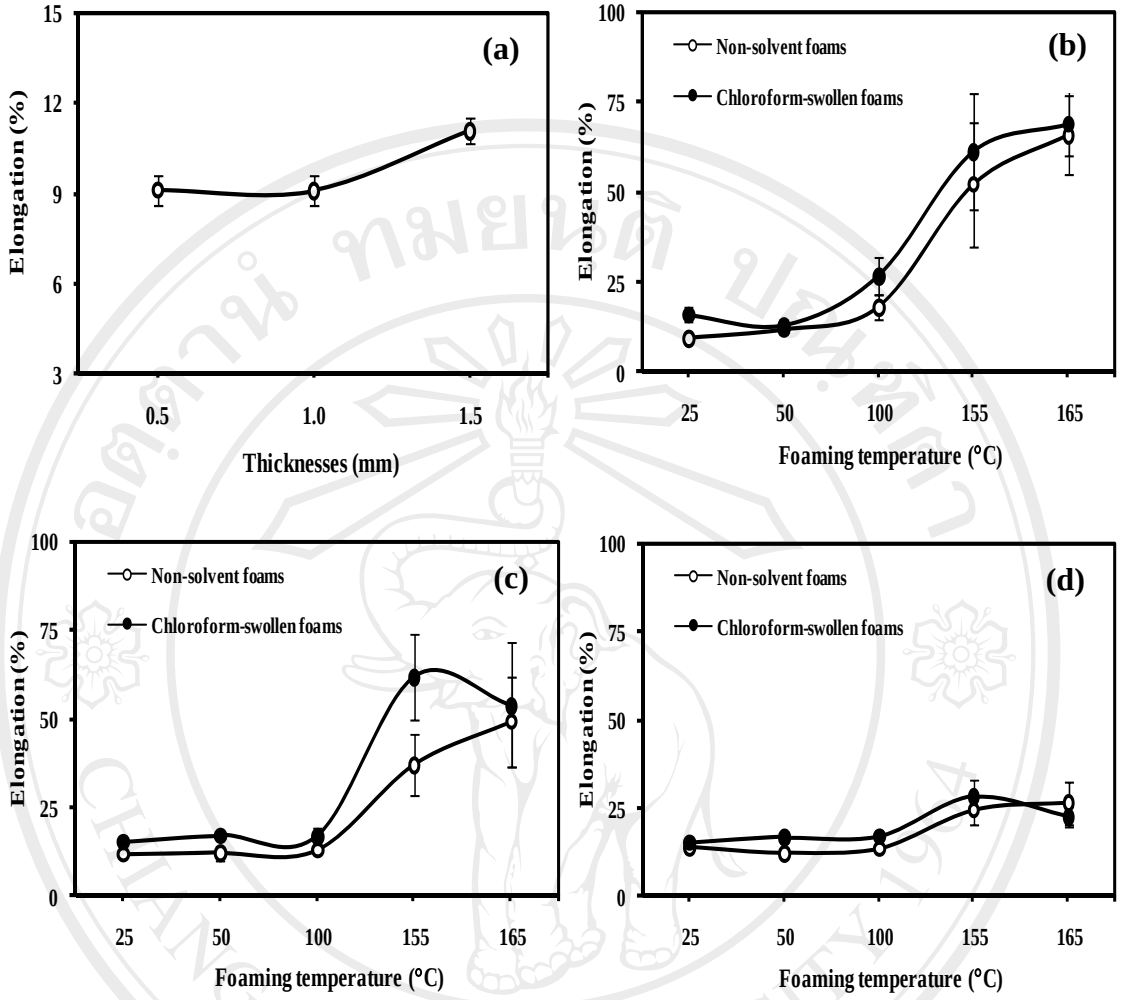

Figure 3.17 Elongation at maximum load of all samples at various foaming temperatures; (a) Un-foamed sheets (b) PP foams with 0.5 mm (c) PP foams with 1.0 mm, and (d) PP foams with 1.5 mm.

Similar to the elongation of un-foamed samples, the samples showed the Young's modulus that was not a function of the sample thickness as shown in Figure 3.18 (a). According to the increment of elongation property, the PP foams provided less modulus values compared to those of the un-foamed samples and they showed the similar tendency for all sample thicknesses. The tensile modulus of the foams was

decreased from 300 MPa to 80 MPa compared to the un-foamed samples for the same thickness and it was decreased as the temperature increased. As mention at the previous part, the resulted values were increased as the density of the foams increased. Moreover, it was speculated that the tensile modulus of cellular material might be attributed to the elongation around the bubbles or cells due to the cell growth [93]. According to such theory, the relative mechanical property of foam can be related to its density by the following equation;

$$\frac{P_f}{P} = C\left(\frac{\rho_f}{\rho}\right)^z \qquad (3.3)$$

Where P_f is any properties of the foam and P is the same property for the bulk (un-foamed) polymer, while the quantities ρ_f and ρ are the densities of foam and bulk polymer, respectively. C is a constant that equal to 1.0 when the property is the modulus and to 0.3 when it is the collapse stress. The exponent z equals to 2 and 3/2 for the modulus and collapse stress, respectively [122]. From the curve of the Young's modulus, the tensile modulus of the foam increased as the density of the foam increased; it could be observed in the non-solvent foams. Namely, the samples which were foamed at low temperature provided more density than that of the foams at high foaming temperature as previously discussed. The non-solvent foams showed the slightly decreasing of the modulus values as the foaming temperature increased as shown in Figure 3.18 (b)-(d). It was found that these foams exhibited the modulus property, accordingly to the theory in the case of the C is 1.0 and z is 2 when foaming without the solvent-swelling step. At low temperature, the non-solvent foams gave the modulus values near the values of the un-foamed samples at all thicknesses. The values of non-solvent foams decreased as the foaming temperature increased due to

the foaming temperature facilitated a high void fraction then the void fraction promoted the density reductions of the foams. Although, the foaming temperature was counted as a factor on the foam property at high temperature of foaming but in the case of non-solvent foams, the polymer sheets were not treated by the solvent; therefore, the cell nucleation of the non-solvent foams was influence only by the foaming temperature. Again, it was known that the cellular morphology of the foams was strongly depended on the processing conditions. Therefore, when the polymer sheets were processed with the different conditions then the final foams would promote the various formations of the cellular structure. It could be seen in the case of foaming with solvent swelling step. For chloroform-swollen foams, the polymer sheets were treated by the solvent; which also behave as a chemical blowing agent (at high temperature) and a plasticizer (at low and high temperatures) during the process, thus the cell nucleation of chloroform-swollen foams was affected by both the foaming temperature and the behavior of the solvent in the polymer matrix. Consequently, the change of the modulus values of chloroform-swollen foams could not be theoretically predicted using Equation 3.3 due to their cellular morphology (the change of the modulus was not a function of the density but it was affected by the morphology of the polymer matrix).

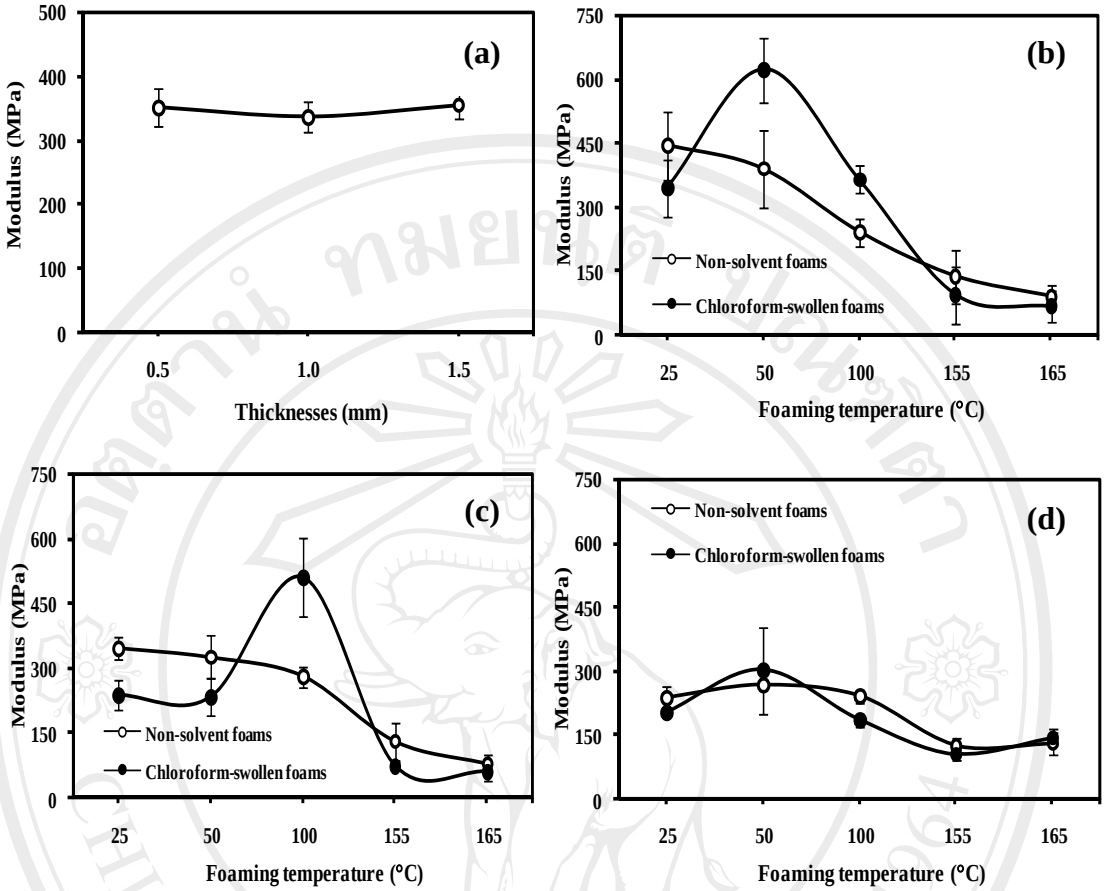

Figure 3.18 Young's modulus of all samples at various foaming temperatures; (a) Un-foamed sheets (b) PP foams with 0.5 mm (c) PP foams with 1.0 mm, and (d) PP foams with 1.5 mm.

3.4.7.2 Impact strength

For the impact testing, the thin samples (i.e., 0.5 mm and 1.0 mm) could not be performed using the testing machine, because the sample was not thick enough according to the requirement of the test. Therefore, it was only 1.5 mm-thick sheets that were foamed and notched for using as the specimens in the experiment. The notched Izod impact properties of PP microcellular foams with 1.5 mm of thickness were measured and calculated relatively to their density in order to gain the specific

impact strength. An increment of impact property of the resulting foams was a function of foaming temperature as shown in Figure 3.19. The foams that processed with and without the chloroform swelling step provided higher specific impact strength than that of un-foamed sheet about 2 to 6 folds. It was clearly seen that the chloroform-swollen foams provided superior impact strength than the non-solvent foams. According to the effect of the foaming temperature that could facilitate the foams with a high void fraction (Figure 3.13) as resulted in the flexibility of the foams. During the testing, the impact energy could be absorbed and distributed all over the polymer matrix through the cellular structure. This made the foams resists to the more impact force and showed the superior impact property than un-foamed samples and also non-solvent foams. Moreover, the fracture characteristics of the samples after impact testing were investigated using the optical stereomicroscope and SEM in order to see the relationship between the impact strength and fracture mode of the samples. The fracture surface images (near the notched area) of the samples were shown in Figure 3.20. It is known that the majority of impact toughness of semicrystalline polymers such as PE and PP are ductile at low strain rates, but at high strain rates such as those experienced in Izod impact test, exhibit a brittle behavior [123]. Yuan *et al*. [123] discovered that the nature of fracture surface morphology of the brittle sample (i.e., neat PP) was different from the ductile sample (i.e., PP-clay nanocomposite which provided the superior impact strength). In the neat PP, the rapid breakdown of the craze initiation zone does not provide adequate time for the material ahead of the initiation zone to respond, resulting in the brittle-like fracture surface. However, the high toughness of the nanocomposite results in slower breakdown of the initiation zone and is characterized by an initial propagation zone, which has a

macroscopically rougher surface than neat PP [123]. After investigation on the fracture surface of the sample, the rougher surface in the wide area of initial propagation zone was observed in the samples (both non-solvent and chloroform-swollen PP foams) which provided high impact strength as shown in Figure 3.20 (b)-(c). While the brittle behavior (crazing surface) was observed in the un-foamed PP sheet as two circle areas as shown in Figure 3.20 (a). Consequently, the macroscopic of the sample was thoroughly investigated and the images showed the matrix ligaments in the propagation zone as the circle area as shown in Figure 3.21 (a)-(b). On comparing, for the fracture behavior of nanocomposites, the reinforcement leads to transformation of the fracture surface from predominantly craze-like and vein-type features to predominantly a combination of micro-void coalescence and fibrillation fracture. It was believed that nanoclay must be the source of micro-void nucleation. Thus the matrix ligaments between these voids are extensively deformed in the propagation zone and leading to a combination of micro-void coalescence and fibrillated fracture. While in the neat PP, only crazing contributes to energy absorption, in general, this could not absorb too much energy resulting in brittle fracture behavior [123-124]. In this research, the PP foams with superior impact strength revealed the matrix ligaments as the fracture behavior of the ductile material as the same reason of the nanocomposite. The increasing in the initiation propagation zone was presented in the fracture surface; it could be summarized to be a ductile nature. For this research, the relationship between the fracture mode and impact strength of un-foamed sample and foamed samples (non-solvent and chloroform-swollen PP foams) was clearly seen and the relationship could be discussed as previously mentioned.

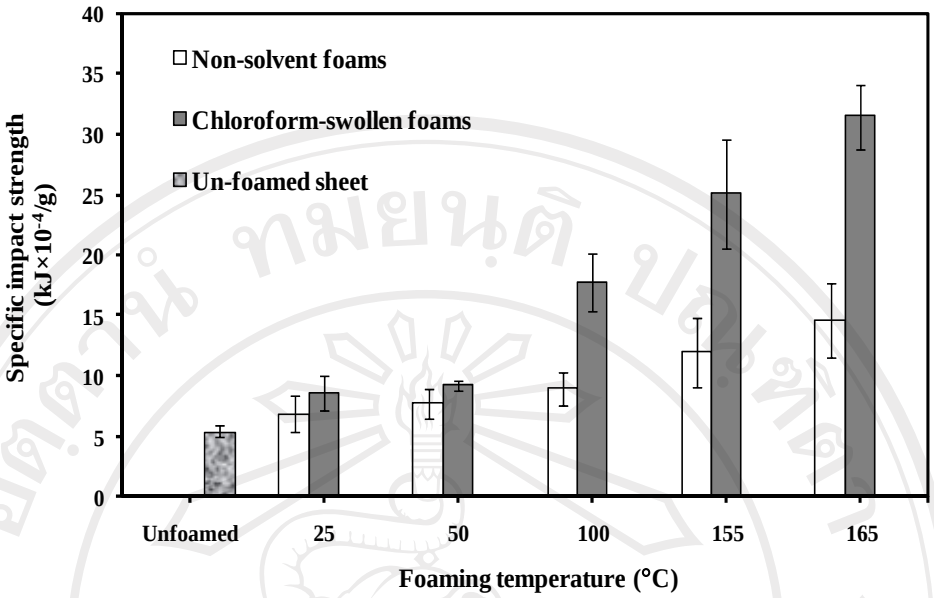

Figure 3.19 Specific impact strength of all samples at various temperatures.

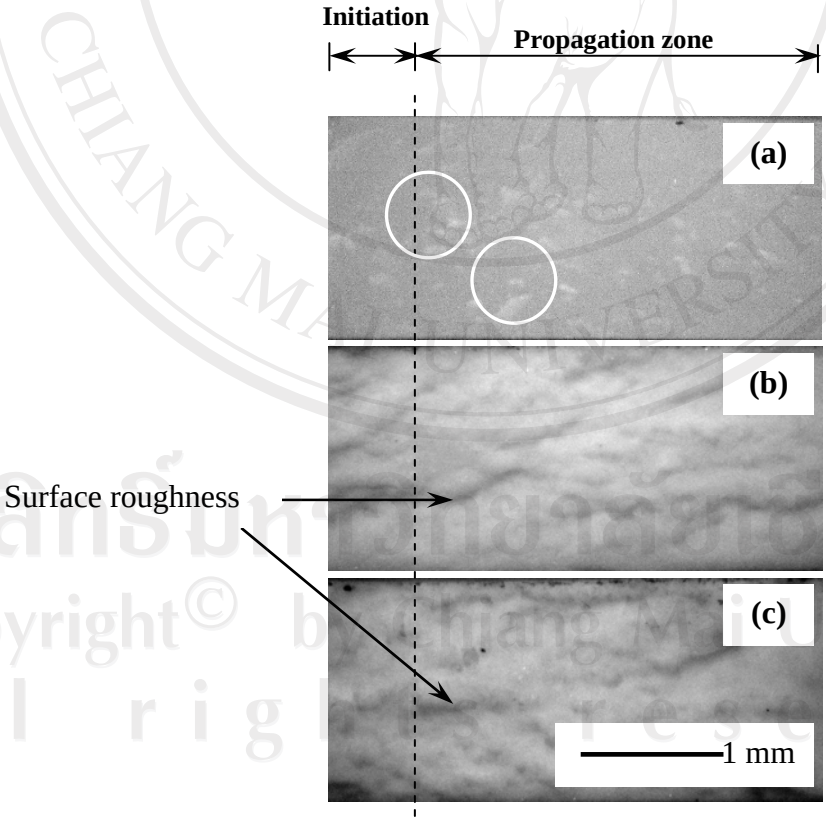

Figure 3.20 Fractography of the samples after impact testing; (a) un-foamed sample, (b) non-solvent and (c) chloroform-swollen PP foams at 165 °C.

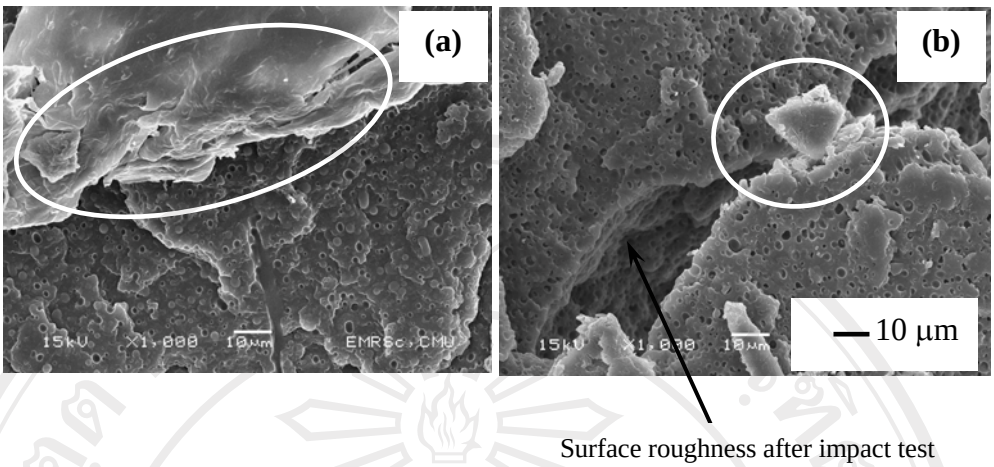

Figure 3.21 Macroscopic (SEM images) of PP foams at 165 °C after impact testing; (a) non-solvent foam and (c) chloroform-swollen foam.

3.5 Conclusions

In this research, the influence of the stiffness phase due to the crystalline fraction of PP was a critical point to encourage improving the processability of PP microcellular foam. Chloroform was selected to swell the polymer matrix prior to the gas saturation step in order to enhance the stiffness loss in the matrix due to the comparable solubility parameter of PP and chloroform. The crystallinity drop evidenced the significant performance of chloroform to allow a high content of gas to be absorbed into the polymer matrix during the process resulted in a high density of nuclei. Whereas to achieve the same amount of cell density, non-solvent samples required a high foaming temperature (near the melting point of the matrix) and the cell coalescence phenomena still appeared in the products. An introduction of solvent plasticization using chloroform as a plasticizer was a profit to generate the microcellular structure in PP matrix for the solid-state batch foaming process as an accomplishment of a high cell density and microcellular foam. Furthermore, the

resulting microcellular foams could be foamed at the ambient by using our strategy. The study of the chloroform-swollen softening effect on foam properties and cellular structure of PP foams exhibited the benefit of chloroform on the foamability. The results showed that the plasticization effect of chloroform could facilitate the foamability of foams, especially at low foaming temperature (25 °C and 50 °C) and it also contributed the cell uniformity of the final foams when foaming at a high temperature (155 °C). However, the solvent performance on final foam was investigated negligibly the thickness of polymer sheet. Thus the thickness effect of the samples was also studied. The performance of chloroform on the foamability and the cellular morphology of PP foams with the different thicknesses (0.5 mm, 1.0 mm, and 1.5 mm) using the solid-state foaming process was observed. The thickness slightly affected on the foamability and cellular structure as the cell nucleation behavior of thin sheet (0.5 mm) was more easily generated than that of a thicker one due to the different heat transfer through the different thickness of PP sheet as clearly seen in the chloroform-swollen foams at low temperatures (25 °C and 50 °C). In addition, the effect of solvent plasticization on the mechanical properties of the microcellular PP foams such as tensile properties and impact strength was also investigated. It was found that when the microcellular structure was generated on PP by including the swelling step in the foaming process the foamed samples possessed superior impact strength compared to those of un-foamed samples and non-solvent foams even the process was done at low temperatures. The relationship between the fracture behavior and impact strength of the samples after impact test was clearly seen. The microcellular structure of the PP foams could act as a toughener in the PP matrix, which provided the ductility and superior impact strength. Although, the tensile

properties of the foams seemed to be lowered than those of the un-foamed samples but more flexible PP products could be accomplished with the interior microcellular structure.